

000
001
002
003
004
005
006
007
008
009
010
011
012
013
014
015
016
017
018
019
020
021
022
023
024
025
026
027
028
029
030
031
032
033
034
035
036
037
038
039
040
041
042
043
044
045
046
047
048
049
050
051
052
053

054
055
056
057
058
059
060
061
062
063
064
065
066
067
068
069
070
071
072
073
074
075
076
077
078
079
080
081
082
083
084
085
086
087
088
089
090
091
092
093
094
095
096
097
098
099
100
101
102
103
104
105
106
107

Supplementary Material for Test-Time Training for Change Detection in Remote Sensing Images

Anonymous CVPR submission

Paper ID 11246

Abstract

In this supplementary material document, we provide additional implementation details of our Test-Time Training for Change Detection in Remote Sensing Images.

1. Additional Details on PCC

Polynomial color correction has been originally used in device characterization. In CD, we adopt this concept to map pre-change color space to post-change color space so that resulting difference image \mathbf{I}_d is less sensitive to isolated radiometric changes in pre-change and post-change images. Suppose that, we have N color samples from the post-change image, the corresponding camera response $i_1, i_2, i_3, \dots, i_b$ (where b is the total number of color bands) can be represented by a $1 \times b$ vector ρ_n where $n = 1, 2, 3, \dots, N$. If only $i_1, i_2, i_3, \dots, i_b$ values are utilized in ρ_n , the transformation between pre-change and post-change is a simple linear transformation. The idea of PCC is that vector ρ_n can be expanded by adding more terms (i.e., $i_1^2, i_2^2, i_3^2, \dots, i_n^2$), so that better results can be achieved.

1.1. If pre-change and post-change images have only three-bands (R, G, and B):

If the pre-change and post-change images have only three bands (i.e., $b = 3$, and $i_1=R, i_2=G, i_3=B$), we have following polynomial kernel function ρ :

$$\rho = [R, G, B, RB, RG, BG, R^2, G^2, B^2, RGB] \quad (1)$$

1.2. If pre-change and post-change images have four or more-bands

If pre-change and post-change images have four bands (i.e., $b = 4$, and $i_1=R, i_2=G, i_3=B, i_4=Y$), we have following polynomial kernel function ρ :

$$\rho = [R, G, B, Y, RG, RB, RY, GB, GY, BY, R^2, G^2, B^2, Y^2, RGB, RGY, RBY, GBY, RGY] \quad (2)$$

For pre-change and post-change images having more than four bands ($b > 4$), we consider polynomial terms up to third order to construct the kernel function considering the computational complexity of PCC.

1.3. Additional PCC results on OSCD dataset.

Figure 1, shows additional qualitative results on PCC on OSCD dataset [3]. From the figure we can observe that how well the polynomial correction transforms pre-change image color space in to the post-change color space via polynomial regression. This procedure greatly reduces the isolated colorimetric changes between pre-change and post-change images. Therefore, the resulting difference image \mathbf{I}_d is less sensitive to the color shifts between pre-change and post-change images.

Continue on next page...

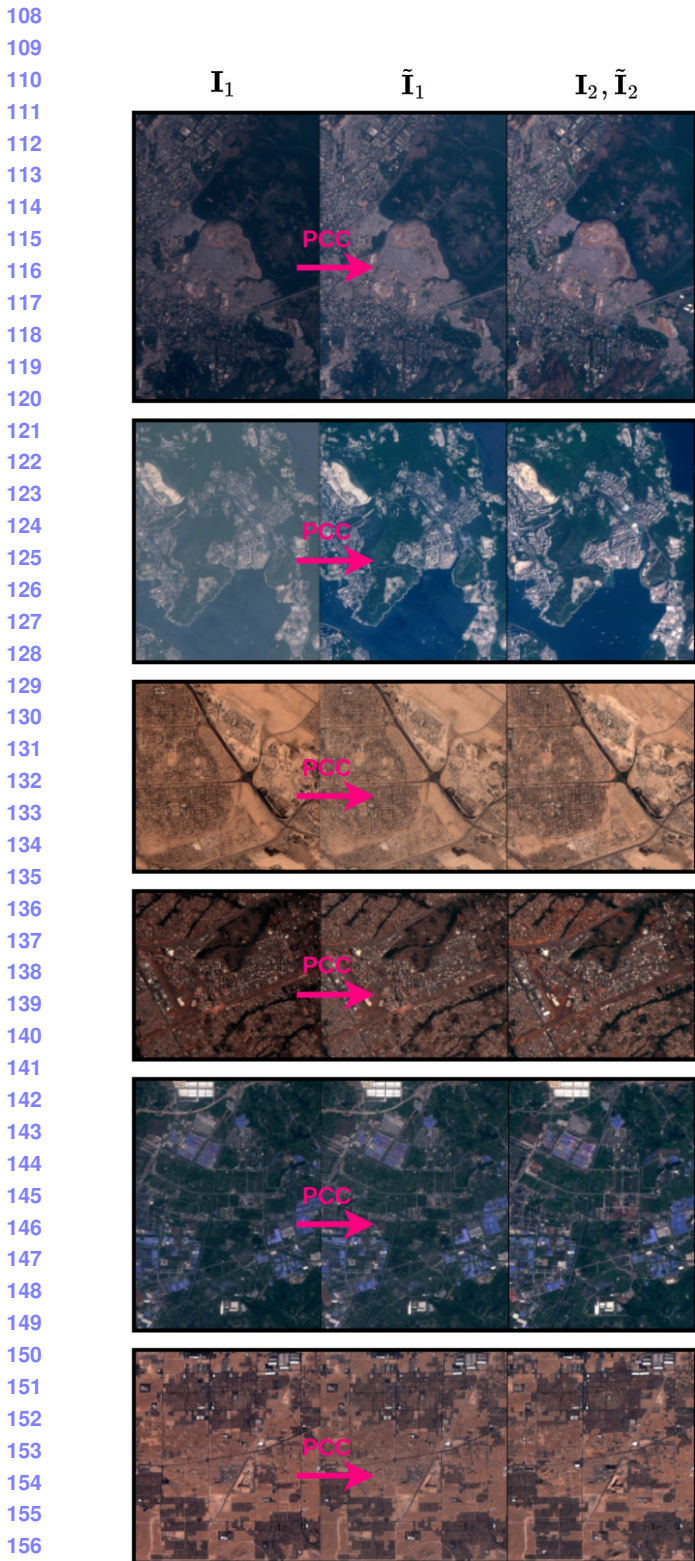


Figure 1. Additional qualitative examples on OSCD dataset [3] to illustrate how PCC maps pre-change image color space to post-change image color space using polynomial regression.



Figure 2. Additional qualitative examples on SZTAKI dataset [1, 2] to illustrate how PCC maps pre-change image color space to post-change image color space using polynomial regression.

216 **2. How our TTT-CD algorithm converges to
217 optimum solution**
218

219 Figure 3, 4, 5, 6, 7, and 8 depict given a pre-change and
220 post-change image pair $\{I_1, I_2\}$, how our proposed TTT-
221 CD algorithm finds the change probability map P_c . The
222 TTT-CD algorithm takes difference image I_d as input and
223 process it through a Deep-Change Probability Generator
224 (D-CPG) to generate the change probability map P_c . The
225 change probability map P_c is used to calculate the the pro-
226 posed unsupervised loss for CD \mathcal{L}_{CD} . We iteratively min-
227 imize \mathcal{L}_{CD} to find the optimal change probability map P_c^*
228 during the testing. Finally, we threshold P_c^* with an appro-
229 priate probability value to obtain binary change map.
230

231
232
233
234
235 **Continue on next page...**
236
237
238
239
240
241
242
243
244
245
246
247
248
249
250
251
252
253
254
255
256
257
258
259
260
261
262
263
264
265
266
267
268
269

270

271

272

273

274

275

276

277

278

279

280

281

282

283

284

285

286

287

288

289

290

291

292

293

294

295

296

297

298

299

300

301

302

303

304

305

306

307

308

309

310

311

312

313

314

315

316

317

318

319

320

321

322

323

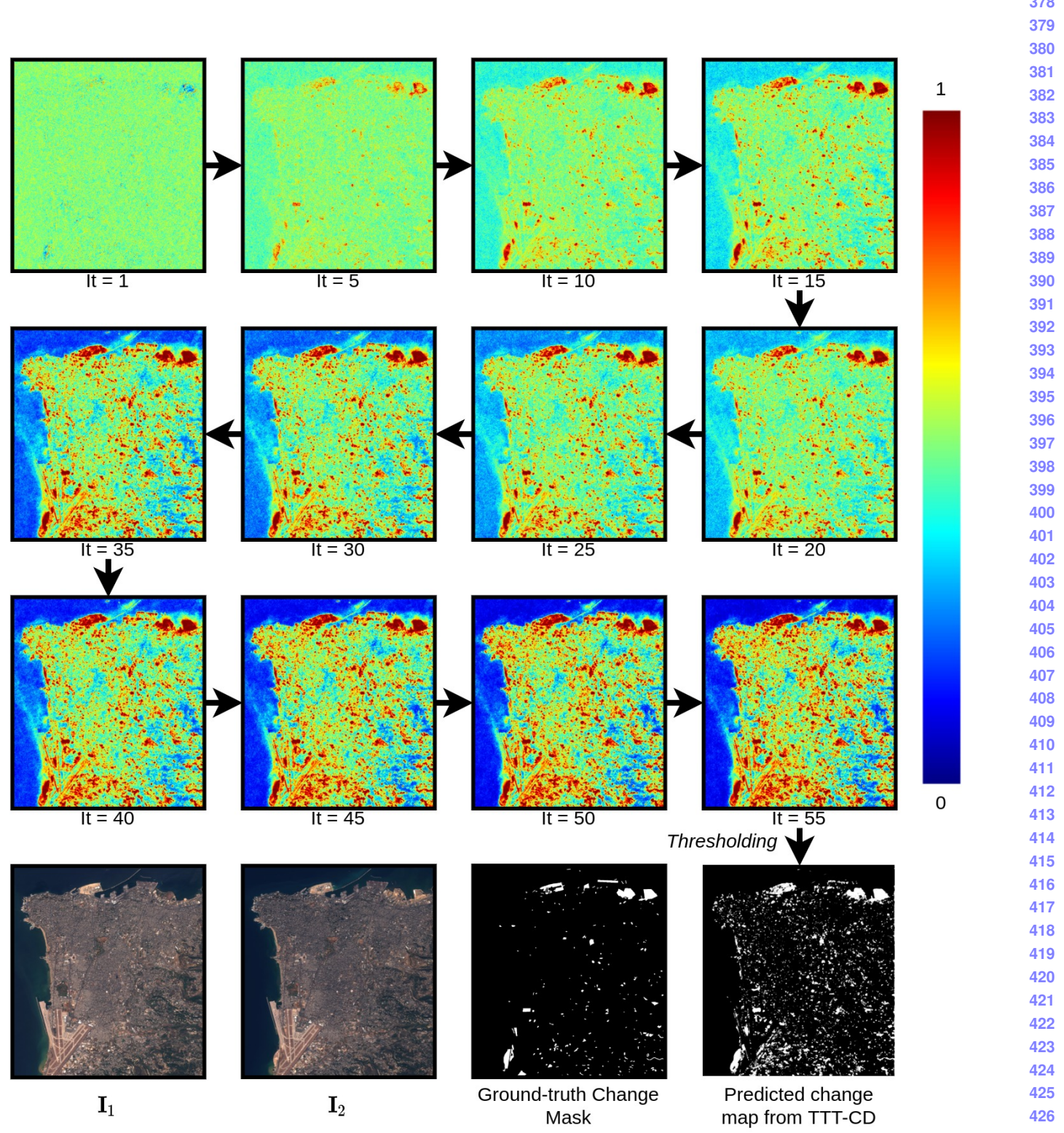


Figure 3. An example on beirut image in OSCD dataset.

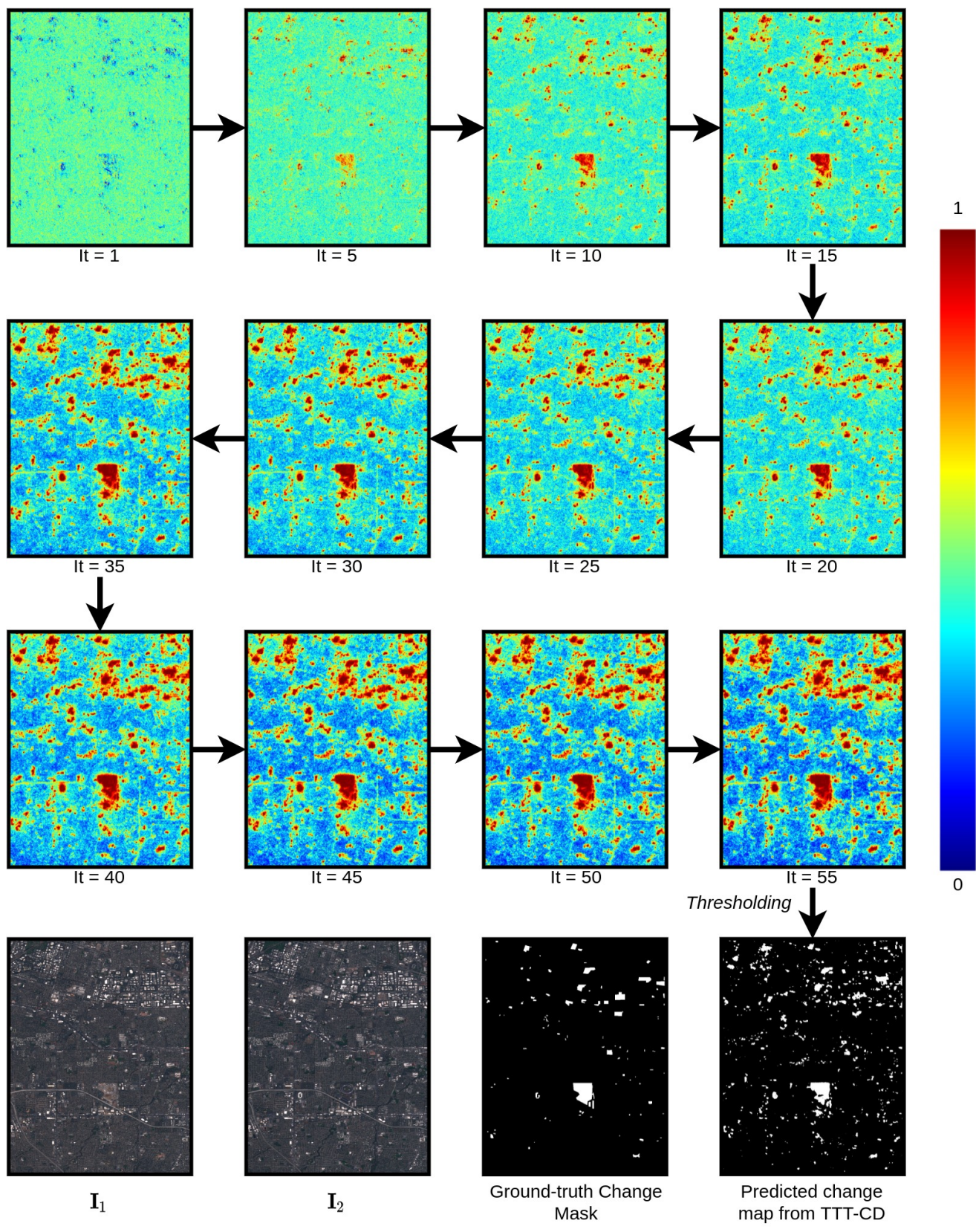


Figure 4. An example on cupertino image in OSCD dataset.

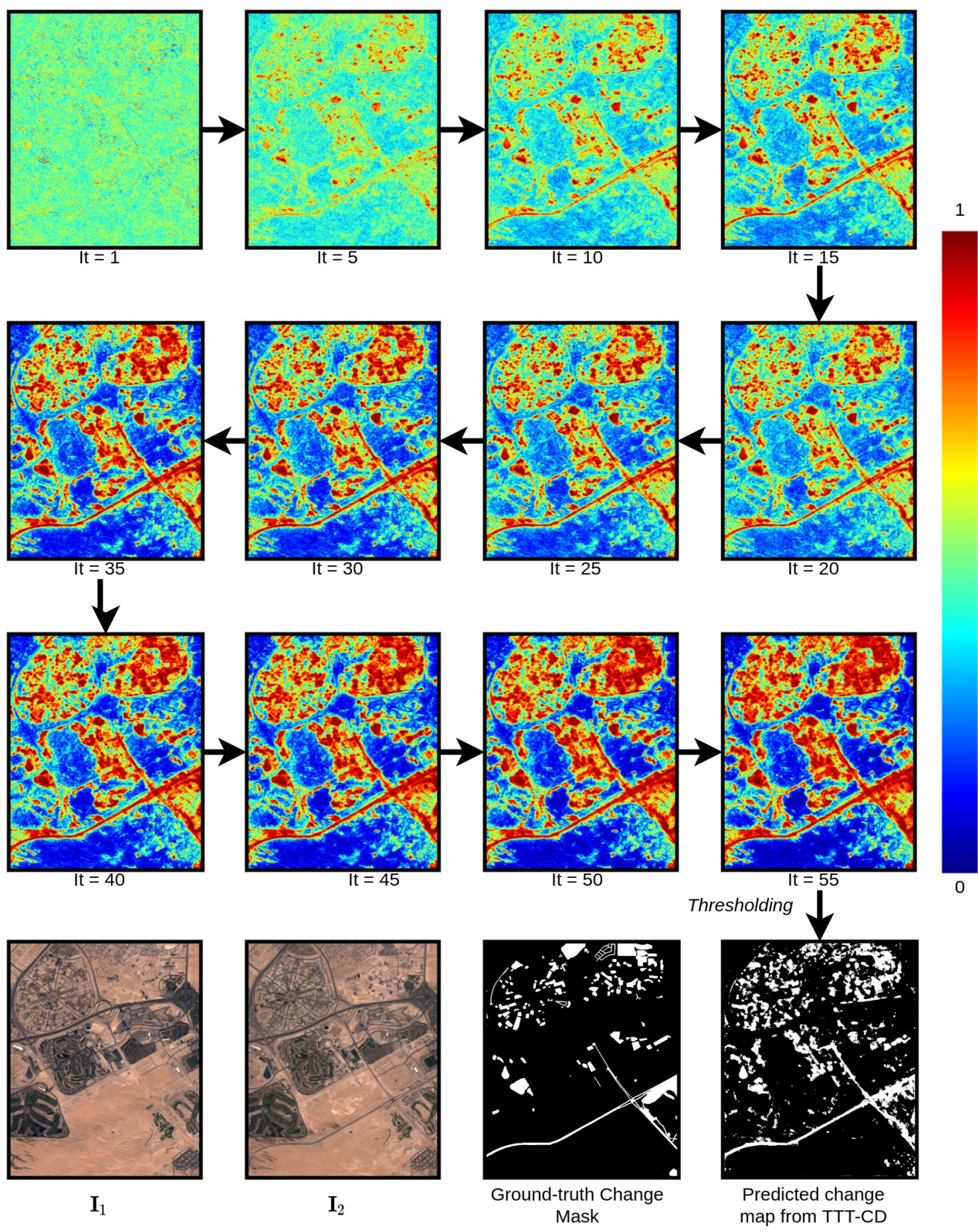


Figure 5. An example on cupertino image in OSCD dataset.

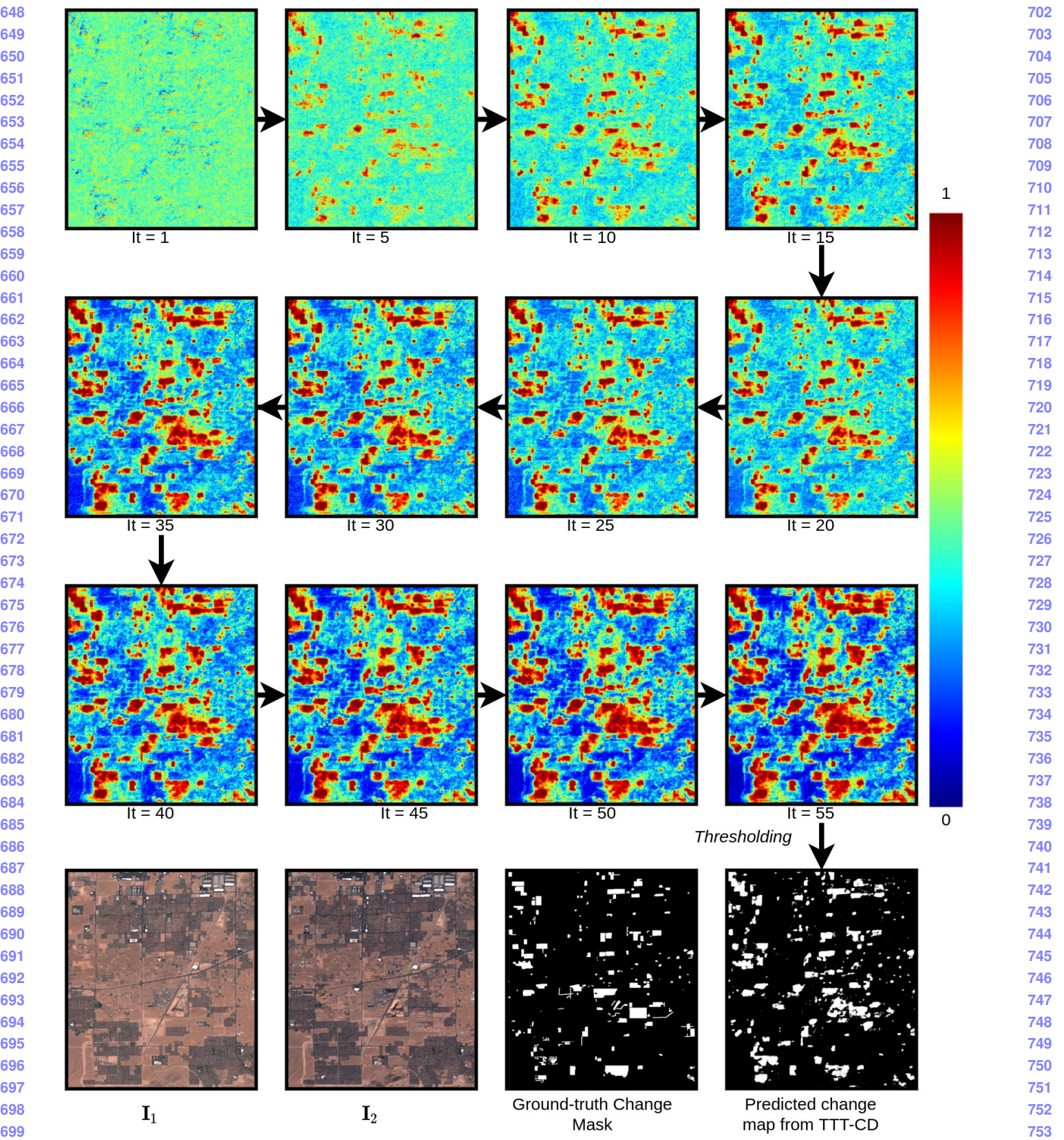
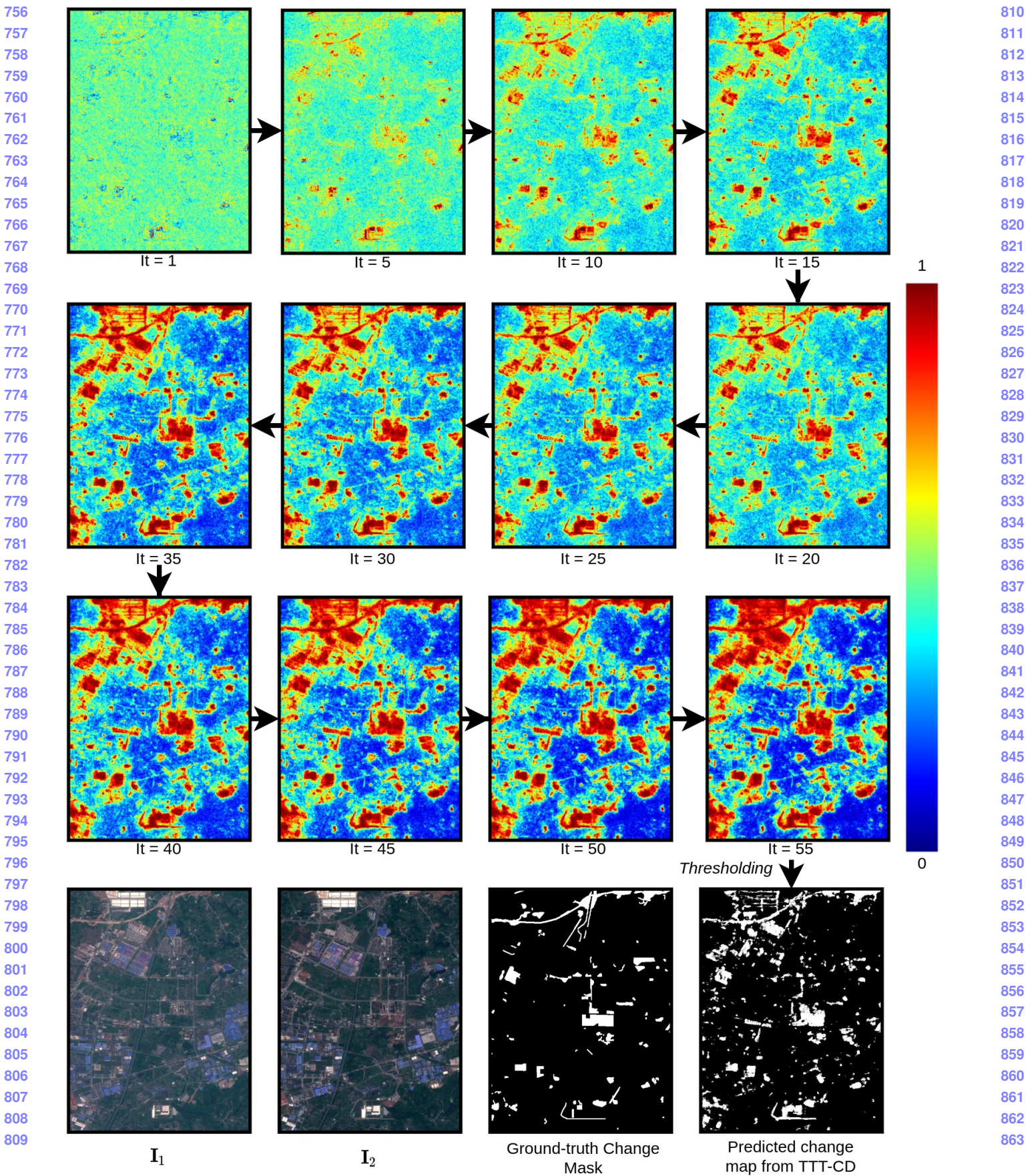


Figure 6. An example on lasvegas image in OSCD dataset.



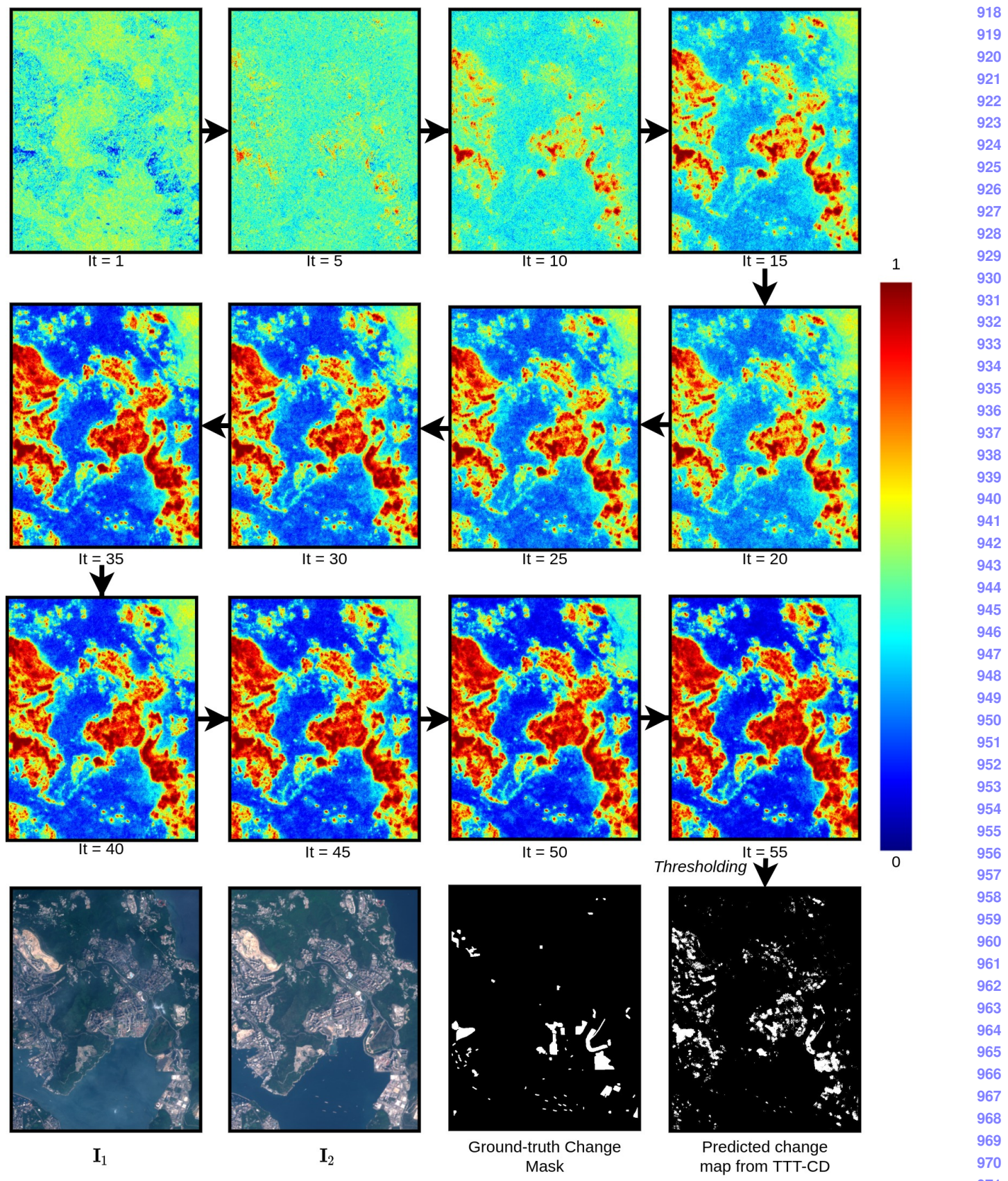


Figure 8. An example on hongkong image in OSCD dataset.

972	3. Additional Qualitative Results on OSCD	1026
973	dataset	1027
974		1028
975	Figure 9, 10, 11, and 8 shows the final change probability	1029
976	map (i.e., difference image) correspond to different SOTA	1030
977	methods on OSCD dataset.	1031
978		1032
979		1033
980		1034
981		1035
982		1036
983	<i>Continue on next page ...</i>	1037
984		1038
985		1039
986		1040
987		1041
988		1042
989		1043
990		1044
991		1045
992		1046
993		1047
994		1048
995		1049
996		1050
997		1051
998		1052
999		1053
1000		1054
1001		1055
1002		1056
1003		1057
1004		1058
1005		1059
1006		1060
1007		1061
1008		1062
1009		1063
1010		1064
1011		1065
1012		1066
1013		1067
1014		1068
1015		1069
1016		1070
1017		1071
1018		1072
1019		1073
1020		1074
1021		1075
1022		1076
1023		1077
1024		1078
1025		1079

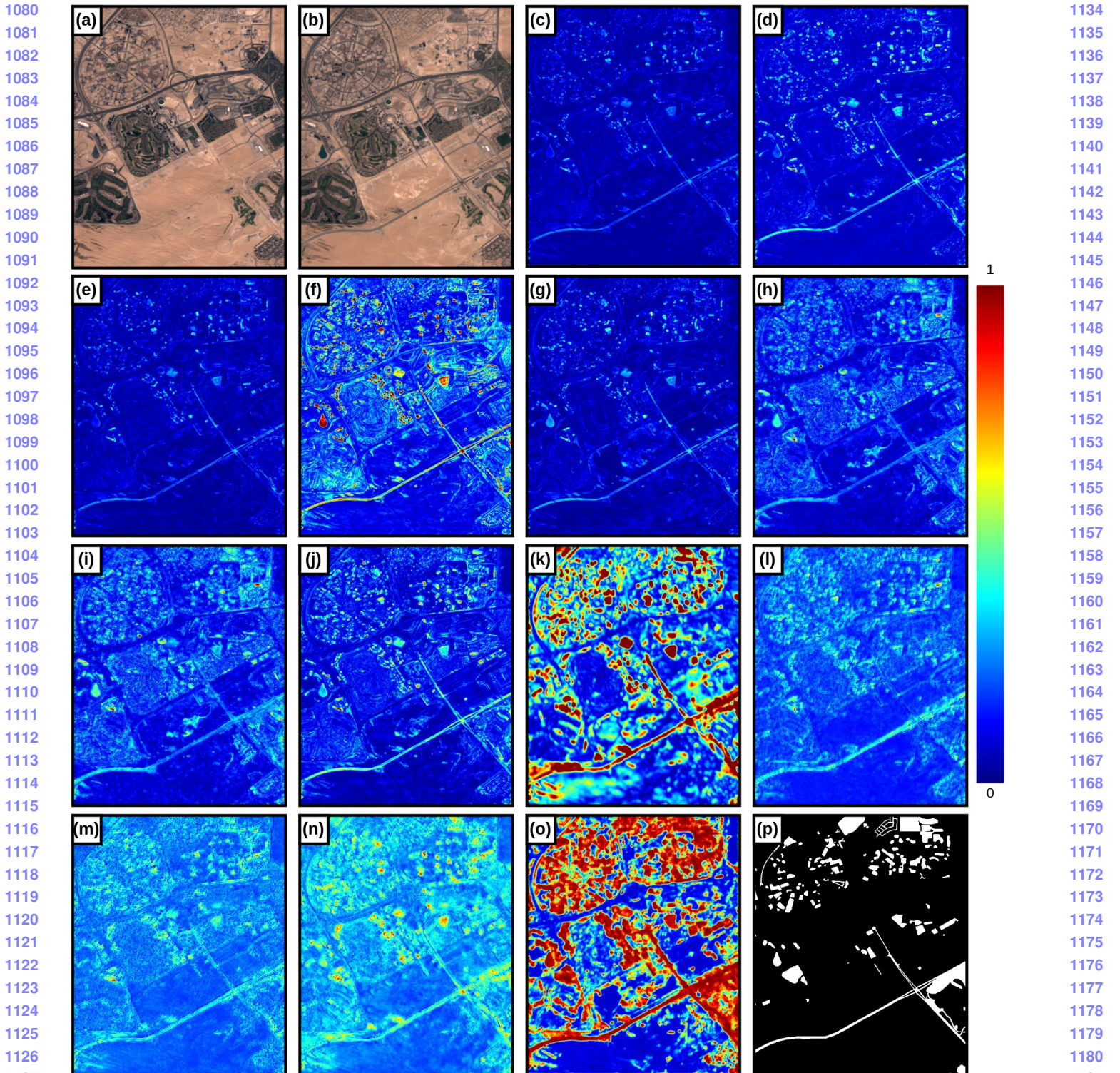


Figure 9. Change probability map (i.e., difference image) of different CD methods for dubai image pair in OSCD dataset. (a) Pre-change image. (b) Post-change image. (c) CVA. (d) DPCA. (e) ImageDiff. (f) ImageRatio. (g) ImageRegr. (h) IRMAD. (i) MAD. (j) PCDA. (k) DeepCVA. (l) UNet. (m) SeCo-Rand. (n) SeCo-Pre. (o) TTT-CD (ours). (p) Groud-truth change mask.

1131

1132

1133

1182

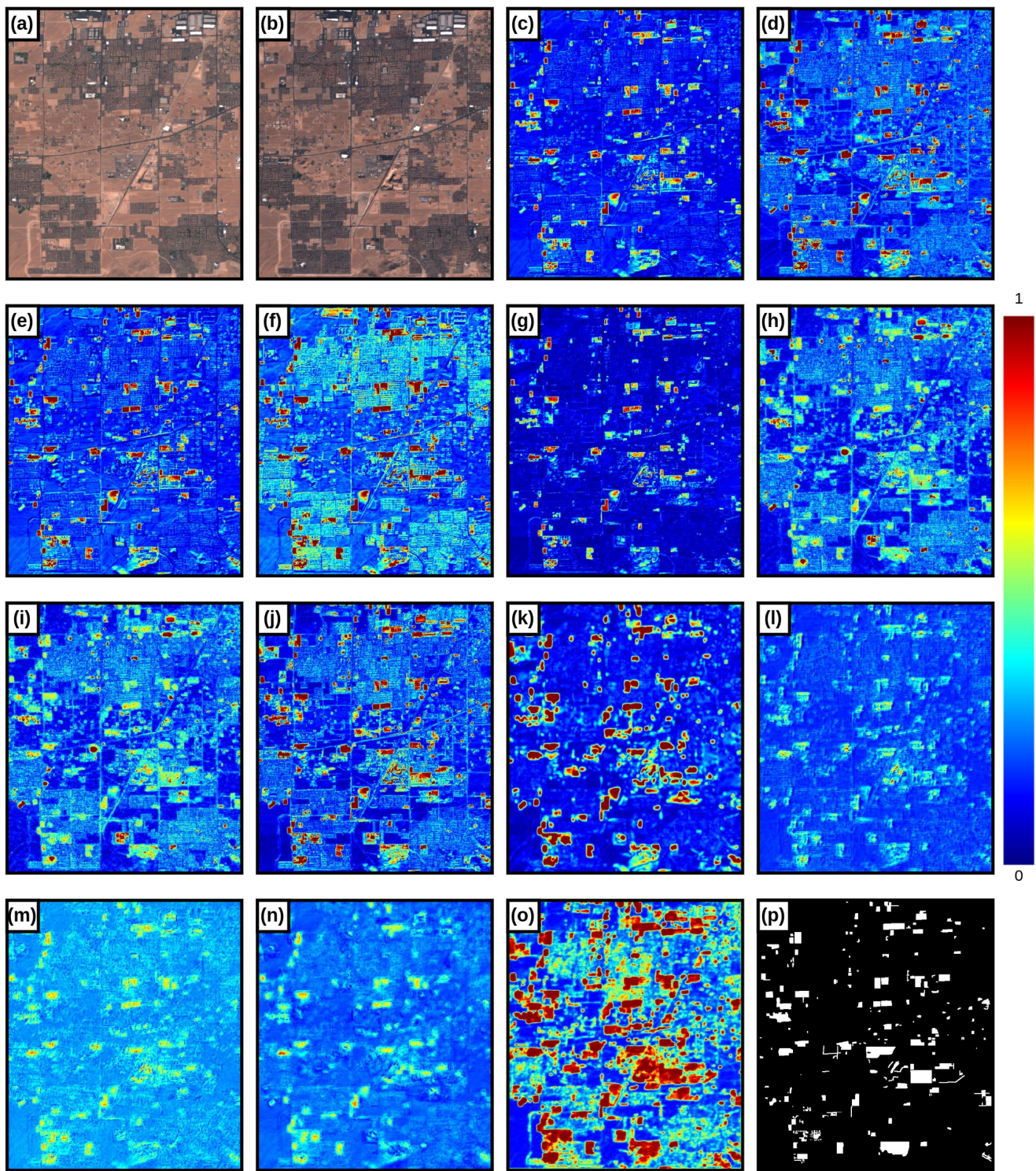
1183

1184

1185

1186

1187

1188
1189
1190
1191
1192
1193
1194
1195
1196
1197
1198
1199
12001201
1202
1203
1204
1205
1206
1207
1208
1209
1210
1211
12121213
1214
1215
1216
1217
1218
1219
1220
1221
1222
1223
12241225
1226
1227
1228
1229
1230
1231
1232
1233
1234
1235
12361237
1238
1239
Figure 10. Change probability map (i.e., difference image) of different CD methods for lasvegas image pair in OSCD dataset. (a) Pre-
1240
1241
change image. (b) Post-change image. (c) CVA. (d) DPCA. (e) ImageDiff. (f) ImageRatio. (g) ImageRegr. (h) IRMAD. (i) MAD. (j)
1242
1243
1244
1245
1246
1247
1248
1249
1250
1251
1252
1253
1254
1255
1256
1257
1258
1259
1260
1261
1262
1263
1264
1265
1266
1267
1268
1269
1270
1271
1272
1273
1274
1275
1276
1277
1278
1279
1280
1281
1282
1283
1284
1285
1286
1287
1288
1289
1290
1291
1292
1293
1294
1295

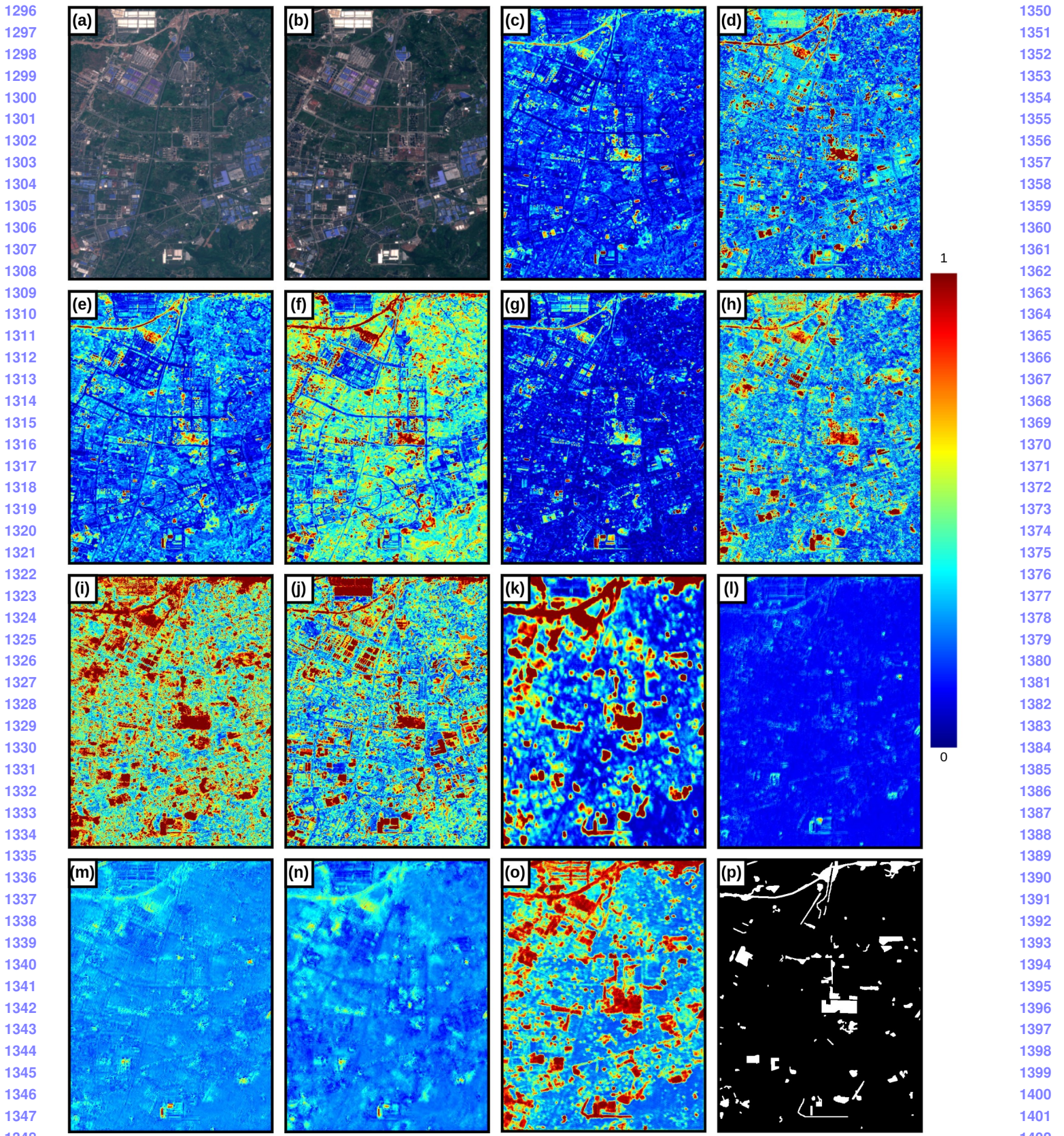


Figure 11. Change probability map (i.e., difference image) of different CD methods for chongqing image pair in OSCD dataset. (a) Pre-change image. (b) Post-change image. (c) CVA. (d) DPCA. (e) ImageDiff. (f) ImageRatio. (g) ImageRegr. (h) IRMAD. (i) MAD. (j) PCDA. (k) DeepCVA. (l) UNet. (m) SeCo-Rand. (n) SeCo-Pre. (o) TTT-CD (ours). (p) Groud-truth change mask.

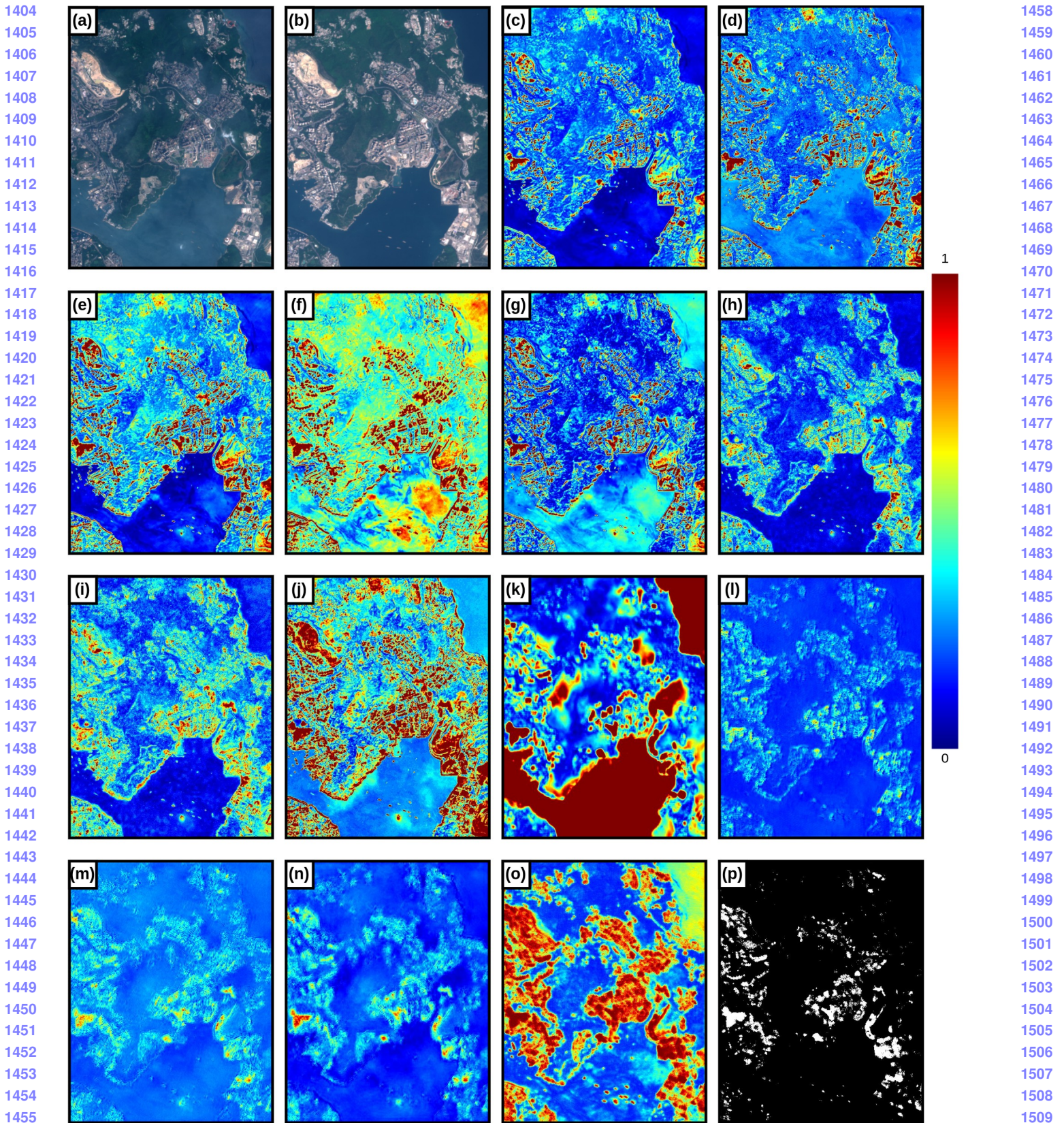


Figure 12. Change probability map (i.e., difference image) of different CD methods for hongkong image pair in OSCD dataset. (a) Pre-change image. (b) Post-change image. (c) CVA. (d) DPCA. (e) ImageDiff. (f) ImageRatio. (g) ImageRegr. (h) IRMAD. (i) MAD. (j) PCDA. (k) DeepCVA. (l) UNet. (m) SeCo-Rand. (n) SeCo-Pre. (o) TTT-CD (ours). (p) Groud-truth change mask.

1512	4. Reproducing Results (Demo)	1566
1513		1567
1514	1. Create a virtual conda environment using the provided	1568
1515	environment.yml (you may use: conda env create -f	1569
1516	environment.yml).	1570
1517		1571
1518	2. Once the environment is setup, open Demo_OSCD	1572
1519	from jupyter notebook and simply run the file.	1573
1520		1574
1521	3. GitHub repository will be made publically available	1575
1522	after the review process.	1576
1523		1577
1524		1578
1525		1579
1526		1580
1527		1581
1528		1582
1529		1583
1530		1584
1531		1585
1532		1586
1533		1587
1534		1588
1535		1589
1536		1590
1537		1591
1538		1592
1539		1593
1540		1594
1541		1595
1542		1596
1543		1597
1544		1598
1545		1599
1546		1600
1547		1601
1548		1602
1549		1603
1550		1604
1551		1605
1552		1606
1553		1607
1554		1608
1555		1609
1556		1610
1557		1611
1558		1612
1559		1613
1560		1614
1561		1615
1562		1616
1563		1617
1564		1618
1565		1619

1620	References	1674
1621		1675
1622	[1] Csaba Benedek and Tamás Szirányi. A mixed markov model	1676
1623	for change detection in aerial photos with large time differ-	1677
1624	ences. In <i>2008 19th International Conference on Pattern</i>	1678
1625	Recognition, pages 1–4. IEEE, 2008. 2	1679
1626	[2] Csaba Benedek and Tamás Szirányi. Change detection in op-	1680
1627	tical aerial images by a multilayer conditional mixed markov	1681
1628	model. <i>IEEE Transactions on Geoscience and Remote Sens-</i>	1682
1629	<i>ing</i> , 47(10):3416–3430, 2009. 2	1683
1630	[3] R. Caye Daudt, B. Le Saux, A. Boulch, and Y. Gousseau. Ur-	1684
1631	bani change detection for multispectral earth observation using	1685
1632	convolutional neural networks. In <i>IEEE International Geo-</i>	1686
1633	<i>science and Remote Sensing Symposium (IGARSS)</i> , July 2018.	1687
1634	1 , 2	1688
1635		1689
1636		1690
1637		1691
1638		1692
1639		1693
1640		1694
1641		1695
1642		1696
1643		1697
1644		1698
1645		1699
1646		1700
1647		1701
1648		1702
1649		1703
1650		1704
1651		1705
1652		1706
1653		1707
1654		1708
1655		1709
1656		1710
1657		1711
1658		1712
1659		1713
1660		1714
1661		1715
1662		1716
1663		1717
1664		1718
1665		1719
1666		1720
1667		1721
1668		1722
1669		1723
1670		1724
1671		1725
1672		1726
1673		1727